



# RAIN HEIGHT INFORMATION FROM MICRO RAIN RADAR AND TRMM PRECIPITATION RADAR FOR COMMUNICATION STUDIES OVER RAYALASEEMA, ANDHRA PRADESH

<sup>1</sup>B.Rohini, <sup>2</sup>Mohammed Waaz, <sup>3</sup>C.V.Krishna Reddy and <sup>4</sup>K.Krishna Reddy

<sup>1</sup>Research Scholar, <sup>2</sup>Assistant Professor, <sup>3</sup>Professor, <sup>4</sup>Professor

<sup>1,3</sup>Department of Physics, Rayalaseema University, Kurnool, India

<sup>2</sup>Department of Physics, Silver Jubilee Government College, Cluster University, Kurnool, India

<sup>4</sup>Department of Physics, Yogi Vemana University, Kadapa, India

**Abstract:** One of the key meteorological parameters critical for estimating fade margins for digital microwave link availability in the satellite-Earth propagation path is the 0°C isotherm height or the rain height. Although, ITU-R P. 839-3 recommendation provided a global map of this height in the form of contours at a resolution of 1.5° by 1.5° in both latitude and longitude in regions of the world where no location-specific information is available. However, the precipitation structure depends on the different climatic regions, which makes rain height to be strongly dependent on the local weather. In this report, we present information on rain characteristics of 0°C isotherm height in a semi-arid region of India based on 3 years of precipitation data obtained from the Micro Rain Radar, PARSIVEL Disdrometer, Tipping Rain Gauge, Tropical Rain Measuring Mission (TRMM) satellite. Special campaigns at Kadapa GPS radiosonde and also Hyderabad radiosonde data are utilized for characterizing the melting layer. The analysis has been carried out based on the stratiform rain events which normally exhibit a pronounced melting layer or bright-band. These results are compared with a measurement from ground-based vertically looking micro rain radar (MRR) and the mean 0°C isotherm height provided by the ITU-R P. 839-3 recommendations. It is worth underlining that an annual mean height given by the ITU-R for this region shows an average percentage difference of about 5% of the measured values. This suggests that the fade margin estimated using the ITU-recommended value of this region will be overestimated. Overall, the rain height obtained from TRMM-PR is in agreement with the ground-based MRR. The results also suggest a possible modification in the rain attenuation model taking into account the melting layer height varied with the season and rain rate.

**Index Terms - TRMM-PR, Micro Rain Radar, Radiosonde, Rain Height, Bright-Band Height**

## 1. INTRODUCTION

Increasing demand for broadband multimedia communications coupled with new millimeter-wave spectrum issued by governments throughout the world has motivated extensive research in new wireless services. The design of a high-performance broadband millimeter-wave communication system requires detailed knowledge of radio wave propagation channel. At frequencies above 10 GHz, one must not only consider classical propagation phenomena such as reflection, diffraction, and scattering, but also the interaction of electromagnetic waves with the atmosphere, and particles such as rain, snow, and hail (Crane, 1996), (Freeman, 1987). In the absence of actual slant path attenuation measurements, system designers are often forced to rely on the rain attenuation models. These models are based on certain assumptions and on the measured meteorological parameter in temperate locations. These models are found to be inadequate for attenuation prediction in tropical region due to the different characteristics of rain and other hydrometers (D.N.Rao et al, 1997 and (Propagation data and prediction methods required for design of Earth-space telecommunication systems, 2001).

Satellite communication links operating beyond the 10 GHz frequency range often suffer some level of degradation by hydrometeors like rain, ice, fog, hail, sleet, snow as they propagate through the atmosphere (G. O. Ajayi et al 1990 and D Atlas et al 1973). Among the hydrometeor, rain attenuation is known to be the dominant propagation impairment at such frequency. Attenuation due to rain can either be by absorption or scattering, but the scattering which happens when there is a reflection of the microwave energy out of the communication path by rain drops or a process of interaction between the microwave signal and the

medium in such a way that causes the signals to go in directions different from the intended direction is of more concern to the system designer (ITU-R P.839-3, Rain height for prediction methods, 2005).

In order to make the proper link design calculation, a propagation predictions mechanism must be carried out in the absence of real time attenuation measurement. However, attenuation prediction methods consider among other parameters the mean rain height,  $h_r$ . Although, ITU-R P. 839-3 (Propagation data and prediction methods required for design of Earth-space telecommunication systems, 2001) recommendation provided a global map of this height in the form of contours at a resolution of  $1.5^\circ$  by  $1.5^\circ$  in both latitude and longitude in regions of the world where no location specific information is available. In addition, studies carried out in different tropical regions show location dependent as well as seasonal variation of rain height, which suggests that the value might vary through the year, (U.V.Murali Krishna et al 2014),(G. Peters et al 2002), (J.Jayalakshmi et al 2014) and (M. Thurai et al 2005). Studies on rain height based on radar reflectivity has attracted the attention of many researchers in the tropics among are (J. W. Cha et al 2007, W. Klaassen 1988, G. Galati 1996, D.N.Rao et al 1994, J.Janapati et al 2020). They observed variations in the rain height in all the stations considered and concluded that a fixed value cannot be assigned to the entire region.

One of the globally used models for calculation of attenuation is ITU-R model P. 618-9 (Propagation data and prediction methods required for design of Earth-space telecommunication systems, 2001). This model uses the assumption of a constant rain height for the calculation of effective path length. The rain height is derived from yearly averaged zero degree isotherm height. But, in tropics, it is found that the rain height is not invariant with time, and shows significant variation with the rain rate (G. O. Ajayi et al 1990). Therefore, the aim of this paper is to emphasize on difference between measured rain attenuation in tropical semi-arid region, Kadapa, India, and ITU-R predictions and results may also be extrapolated for use in tropical regions that have similar situation as the Rayalaseema region; also, the study will be helpful for understanding the rain attenuation characteristics over the Indian tropical region.

## 2. EXPERIMENTAL SETUP AND DATABASE

This section, briefly discusses different meteorological instruments used, data collection and methodology adopted in this work. The YVU campus outdoor meteorological station is a monitoring instrument used to monitor real-time environmental changes and make corresponding warnings. Usually used in the meteorological industry. With the rise of various industries, automatic weather station technology has become more and more advanced and its applications have become more and more extensive. The Meteorological station as shown in Fig.1 is a facility with different equipment intended to punctually measure and record different meteorological variables, such as air temperature, atmospheric pressure, rainfall, relative humidity and wind direction, among others, for different usages, including weather forecasting and Rain drop size distribution (DSD) using PARSIVEL disdrometer, and vertical profiles of DSD using Micro Rain Radar(MRR).



**Fig.1:** Photograph showing Atmospheric Laboratory at Yogi Vemana University, Kadapa. Ground-based PARSIVEL Disdrometer (PSD), AWS, Micro Rain Radar (MRR) and Lightning Sensor (LS). (Inset shows photograph of PSD, AWS, MRR and LS).

### 2.1 MRR DESCRIPTION AND DATA ANALYSIS:

The vertical profiles of rain parameters were observed using micro rain radar (MRR). The MRR is a vertically pointing FM-CW (Frequency Modulated Continuous Wave) Doppler radar and it operates with an electromagnetic radiation at a frequency of 24.1 GHz with a modulation of 1.5 - 15 MHz depending on the height resolution. The outdoor unit of the MRR which comprises of the dish antenna and the radar receiver unit are mounted on the pole placed besides the old Science building at the Yogi Vemana University, Kadapa, India. Also, the indoor unit which made up of the RS 232 data transmission interface and personal computer (PC) based software are installed inside the radio and satellite communication research laboratory (RSCRL) in the department for online control, data visualization, transfer and storage. Fig. 2 shows the outdoor and the indoor unit of the MRR.



**Fig.2:** Experimental set-up showing (a) the Outdoor Unit and (b) indoor unit of the MRR

The MRR has an instantaneous measurement at every 10-s integrated over 1-min with a vertical resolution of 200 m. The 200 m resolution is taken to accommodate the nearly complete profile of the rain up to 6000 m (above the melting layer/bright band over tropical India during all seasons) over this region with a total of 30 range gates. The MRR generates a height range resolved Doppler spectrum. The data processing is performed by a Radar Control and Processing Device (RCPD) which is placed in housing directly below the antenna support. The measured data are transmitted by a serial RS-232 port rate from the outdoor unit. This port connects the MRR to a PC; hence the control, the calculation of further values, and the recording of the data can be done with the MRR-control program. The vertical profile of drop size distribution (DSD) parameters is estimated from the Doppler spectra. Once DSD has been measured with Doppler principle, other rain integral parameters can be obtained. Retrieval of Doppler spectra and different micro physical parameters can be found in details by (Atlas et al, 1993) and (Strauch, 1976) and (Peters et.al.2002).

## 2.2 AUTOMATIC WEATHER STATION (AWS):

An automatic weather station (AWS) is an automated version of the traditional weather station, either to save human labour or to enable measurements from remote areas. An AWS will typically consist of a weather-proof enclosure containing the data logger, rechargeable battery, telemetry (optional) and the meteorological sensors with an attached solar panel or wind turbine and mounted upon a mast. The specific configuration may vary due to the purpose of the system. An AWS works by measuring atmospheric conditions and transmitting them to a network, forecaster, or display. The specific configuration may vary due to the purpose of the system. AWS provide data for air temperature, visibility, wind speed and direction, sea level pressure, humidity, dew point (the temperature to which air must be cooled at constant atmospheric pressure for water vapor to condense into water), and precipitation amount and intensity. In AWS, a Tipping Bucket Rain Gauge (TBRG) is employed, which also has an aperture of 203 mm. An achievable observing accuracy of 5% to 10% is considered to be excellent. Accuracy can be improved by surrounding the rain gauge with a proper windshield.

## 2.3 TRMM-PR DESCRIPTION AND DATA ANALYSIS:

The launching of a satellite known as Tropical Rain Measuring Mission (TRMM) satellite on November 22, 1997 by the National Aeronautics and Space Administration (NASA) of America in collaboration with Japan Aerospace Exploration Agency (JAXA) brought a limelight to the study of precipitation in the tropical and subtropical region. The satellite has been in orbit for more than seventeen years since its launched year. The precipitation radar (PR) on board the satellite has produced an immense amount of information on rainfall patterns within the  $+35^{\circ}$  to  $-35^{\circ}$  latitude range, corresponding to the satellite orbit coverage (D.N.Rao et al 1994).

After the launched, a retrieval algorithm (2A23 PR qualitative) that is applied to the radar observation among whose outputs are the ZDI and bright-band heights was derived by a team of scientists led by (G. Galati et al 1996). For the purpose of this study, we used 3-years (2009 – 2011) TRMM PR level 2 (TRMM 2A23) dataset for the ZDI height and the bright-band to deduce rain height over Kadapa. The reason is to make a comparison with measurement from ground-based vertically looking MRR at this location. For the sake of clarity, we briefly described how data obtained from PR-2A23 are analyzed. Detailed descriptions can be found in (D.N.Rao et al 1991) and (D.N.Rao et al 1994). The Precipitation Radar (PR) Qualitative algorithm (2A23) produces a rain/no rain flag based on echo structure. The algorithm classifies rain type into two different methods: the vertical profile method (V-method), and the horizontal pattern method (H-method). Both methods classify rain into three categories, namely Stratiform, convective, and other details are discussed in (D.N.Rao et al 1994). In the estimation of the Freezing level height, a positive value is the height of the ZDI or bright-band height above mean sea level as the case may be, estimated from the climatological surface temperature data with values expressed in meters, m. If rain is present, the algorithm will detect the bright-band, determine the height of the bright-band and the storm and classify the rain type using special characters as presented in Table 1. The bright-band height is then obtained from the peak value of the algorithm outputs at the point when the bright-band is detected.

**Table 1.** 2A23 PR Algorithm Interpretation

Sl.No	Indication value	Description
1	-8888	No rain
2	-5555	When error occurred in the estimation of Height of Freezing Level
3	-9999	Missing value
4	-1111	No bright-band

The rain height information can be obtained indirectly by studying the melting layer height in stratiform rain type. The Stratiform type of rain is characterized by the low rain rate and higher spatial and temporal coverage. It is normally associated with the melting layer, the region where ice crystals start melting into liquid water. So effectively, the melting layer indicates the limit of rain region in Stratiform rain type. Conventionally, the zero degree isotherm height is used for such rain height estimation, which usually matches with the top of melting layer height. The vertical profile of radar reflectivity can detect the melting layer by bright band signature. The melting layer can be easily identified from the vertical radar reflectivity profile as a sharp peak, called bright band (G. Peters et al 2002) due to the presence of water coated ice crystal in this region which has different dielectric constant.

#### 2.4 RADIOSONDE:

In order to study the effect of zero degree isotherm on the atmospheric parameters over Kadapa (14.28<sup>0</sup> N, 78.42<sup>0</sup> E), upper air observations were planned using Dr.Pisharoty GPS radiosondes (Subrahmanyam *et al.*, 2011). The GPS radiosonde is launched every 3 hours during special campaign. For the present study, the important atmospheric parameters such as humidity, pressure, temperature and winds from surface to 30 km height with an altitude resolution of ~10 m (sampled at 2 seconds intervals) were measured for each flight. Later the entire data set has been suitably interpolated to 100 m. Along with these surface observations, we also use the upper air observations, i.e., the radiosonde data, from the Indian Meteorological Department, at Hyderabad (17.4°N,78.2°E), which is spatially about 300 km from Kadapa, at 00:00 and 12:00 GMT (+ 0530 Indian Standard Time, IST). The radiosonde provides vertical profiles of different meteorological parameters (temperature, pressure, humidity, etc.) during the observational period (ascent time). The temperature accuracy is less than 1 K.

#### 2.5 DATA ANALYSIS:

Precipitation shows high spatial and temporal variability. Rain gauges, disdrometers, and Micro Rain radar (MRR) are the tools usually used for measuring precipitation (as shown in Figure 1). Tipping Rain gauge is the most common tool for directly assessing point precipitation at the surface, measuring the depth of rainfall as it accumulates over time. More recently, technologically sophisticated devices such as Micro Rain Radar (MRR) and PARSIVEL disdrometer (PSD) have been used to enhance our knowledge about the composition of precipitation and the potential physical processes underlying its formation. Unlike rain gauges, PSD can detect individual raindrops and measure their size. Knowledge of the drop-size distribution is essential for understanding precipitation processes, estimating rainfall, and improving microphysics parameterizations in numerical cloud models and Radiowave communication studies MRR is another alternative to rain gauges and provides real-time measurement with high vertical and temporal resolution. Micro Rain Radar can also capture the vertical structure of precipitation. Tropical Rainfall Measuring Mission (TRMM) has provided critical precipitation measurements in the tropical and subtropical regions of our planet. The Precipitation Radar (PR) looked through the precipitation column, and provided new insights into tropical storm structure and intensification TRMM precipitation measurements have made critical inputs to tropical cyclone forecasting, numerical weather prediction, radio wave propagation studies and precipitation climatologies, among many other topics, as well as a wide array of societal applications.

Observations with MRR, PSD and AWS were carried out fairly continuously from 01 January 2009 to 31 December 2011. During the observational period, non availability of the data for few days was mainly due to instruments failure, and maintenance. A total of 975 days of MRR, 997 of AWS and 986 days of MRR data are available until 31 December 2011. For the present study 965-days common data from MRR, PSD and AWS is utilization for the precipitation analysis. According India Meteorological Department, the seasons are classified as premonsoon (March, April and May), summer/southwest (S-W) monsoon (June, July, August and September), north-east (N-E)/post-monsoon (October, November and early December) and winter (late December, January and February). In this research work, also the variation of rain height with rain rate for semi-arid region of Kadapa India has been studied by using TRMM data collected during above-mentioned period. During the above mentioned observational period Kadapa-GPS zone special campaign data and IMD Hyderabad radiosonde routine data (<http://weather.uwyo.edu/upperair/sounding.html>) utilized for estimation of 0°C isotherm.

### 3. RESULTS AND DISCUSSION:

#### 3.1 VERTICAL STRUCTURE OF PRECIPITATING CLOUDS AND COMPARISON OF MICRO RAIN RADAR (MRR) OBSERVATIONS WITH TROPICAL RAINFALL MEASURING MISSION (TRMM) OBSERVATIONS:

Precipitation is generally considered to be classified into two different types: Stratiform and convective. To identify the features of drop size distribution (DSD) with these Stratiform and convective precipitation types is mostly used for number of applications (U.V.Murali Krishna et al 2014). Different rain types and seasons are associated with different microphysical dynamics of raindrop spectra, there were number of rain classification schemes proposed by several researchers (J.Jayalakshmi et al 2014), (M. Thurai et al 2005), (J. W. Cha et al 2007), (S. Das et al 2010), (T.N Rao et al 2001).using different ground based instruments like disdrometer, profiler and radar. In the present research, the SW and NE monsoon precipitating clouds are classified into stratiform and convective rainfall, using Micro Rain Radar (MRR). The rainfall is considered as stratiform, if an enhanced reflectivity at the zero degree isotherm (bright band) is observed using MRR. Otherwise it is considered as convective. Figure 3 shows one rainfall event in SW monsoon (11-06-2010) and another in NE monsoon season (30-10-2010) showing melting layer/bright band.

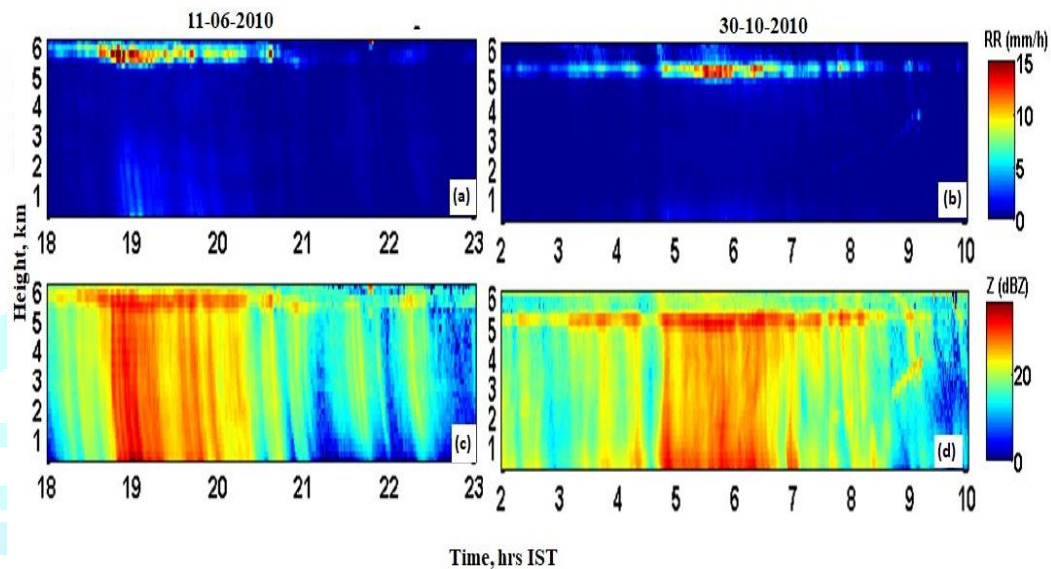


**Fig. 3:** Time-height cross section of Rain Rate (mm/hr) and Radar Reflectivity on 11 June 2010 (SW monsoon) and 30<sup>th</sup> October 2010 (NE monsoon).

Some earlier study revealed that the rain height information can be obtained indirectly by studying the melting layer height in stratiform rain type (D.N.Rao et al 1991), (W Klaassen, 1988) and (S. Das et al 2010). The Stratiform type of rain ( $R \leq 10$  mm/h) is characterized by the low rain rate and higher spatial and temporal coverage. It is normally associated with the melting layer, the region where ice crystals starts melting into liquid water. For the purpose of this work, only the profile rain rate parameter ( $R \leq 10$  mm/h) of the MRR is used while we discarded rain rate  $> 10$  mm/h. For the rain rate parameterizations, we selected the rainy days in all the 3 years of measurement for the analysis. We also classify rain types based on the existence of bright-band signature and the absence of any bright-band in radar reflectivity profile. When there is bright-band signature, the identified rain type is classified as Stratiform ( $R \leq 10$  mm/h), while the convective type ( $R > 10$  mm/h) of rain is characterized by the absence of any bright-band as earlier reported in the following (D.N.Rao et al 1991), (S. Das et al 2010), (F. Fabry et al 1995), (K. Krishna Reddy et al 2003) and (T.N Rao et al 2001). According to (S. Das et al 2010), the bright-band is recognized as the enhanced back scattered part of vertical radar reflectivity profile due to the presence of melting layer. The melting layer has larger reflectivity than the water droplet. It appears like a bright region in the radar reflectivity profile as if heavy rain is occurring at that height. The fact remains that melting layer can only form when there is no strong up-drift, which is only satisfied in Stratiform rain type condition. Hence, the presence of melting layer is a definite symbol of Stratiform type of rain (F. Fabry et al 1995). Any possible error that may arise from the possibility of misidentification of bright-band and which may lead to improper classification of rain were minimized by taking a continuous measurement so that at any random peak is removed in the larger set. Each of the peaks with the identity of the bright-band is then used for the comparison purpose. It is found in an earlier study that the vertical profile of rain rate is more sensitive than radar reflectivity in MRR data product to identify the bright band height (U.V.Murali Krishna et al 2014) and (G. Peters et al 2002). The melting layer top is identified as the height with a maximum negative gradient in rain rate (M. Thurai et al 2005) and (J. W. Cha et al 2007). An example of melting layer observations by MRR is shown in Fig. 4.

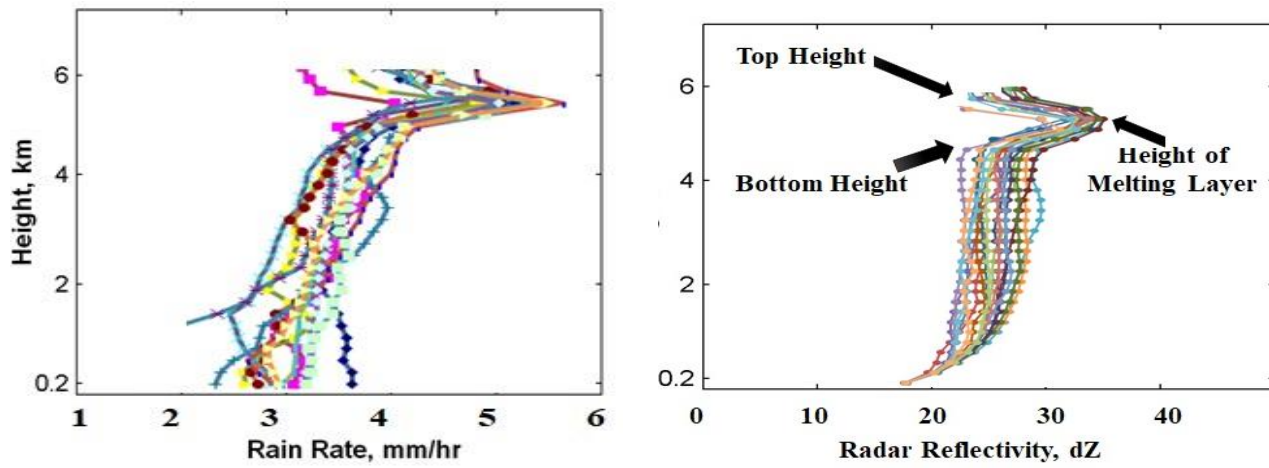


**Fig. 4:** Vertical profiles of (a) Rain Rate, mm/hr and (b) Radar Reflectivity, dBZ representing the melting layer/Bright Band around 5 km height, calculated from instantaneous melting layer information on 9 July 2009.

From the 3 years MRR measurements, data corresponds to rain rate value less than 0.1 mm/h at ground has been discarded because it may contain ground echo. Also, rain rate above 10 mm/h is not taken in to account to consider only the certain cases of Stratiform rain type (W Klaassen, 1988). Data have also been discarded if vertical profile of rain rate is found to be discontinuous at some height as a precautionary measure. Afterward, bright band top height has been determined as the maximum negative gradient of rain rate from the processed data set.

When discussing the vertical structure of precipitation, it is important measurement for the radiowave propagation. Figure 5 shows the monthly occurrence of height of the melting layer/bright band and occurrence percentage of (all cloud fractions) convective clouds, and stratiform clouds observed during January 2009 to December 2011.

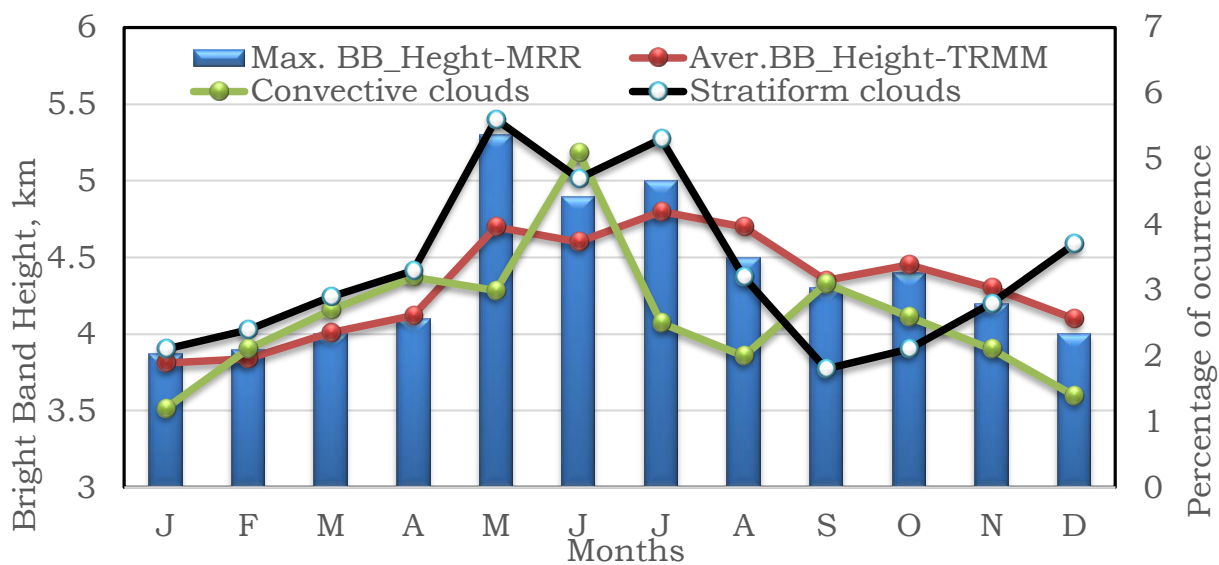


**Fig.5:** Monthly occurrence of height of the melting layer/bright band and Occurrence percentage of Convective clouds, and stratiform clouds observed during January to December 2006. Bright band height observations from Micro Rain Radar (indicates as bar, maximum height of the Bright Band) and also from Tropical Rainfall Measuring Mission (indicated as dash with open square symbol).

**3.2. MONTHLY VARIATION OF RAINFALL, TEMPERATURE:**

In Kadapa, the climate here is considered to be a semi-arid (local steppe) climate with a little rainfall throughout the year. As shown in Fig.6, in Kadapa, the average annual temperature is 28.4 °C and precipitation here is about 606 mm per year. As per figure 5, May is the warmest month of the year. The temperature in May averages 33.4 °C. December has the lowest average temperature of the year. It is 23.8 °C. There is a difference of 129 mm of precipitation between the driest and wettest months. During the year, the average temperatures vary by 9.6 °C. In May the highest number of daily hours of sunshine is measured in Kadapa on average. In May there is an average of 11.26 hours of sunshine a day and a total of 349.13 hours of sunshine throughout May. In January, the lowest number of daily hours of sunshine is measured in Kadapa on average. In January there are an average of 6.91 hours of sunshine per day and a total of 214.14 hours of sunshine. Around 3375.81 hours of sunshine are counted in Kadapa throughout the year. On average there are 111.05 hours of sunshine per month. The month with the highest relative humidity is October (69.44 %). The month with the lowest relative humidity is March (41.50 %). The driest month is February, with 3 mm of rain. With an average of 132 mm, the most precipitation falls in October.

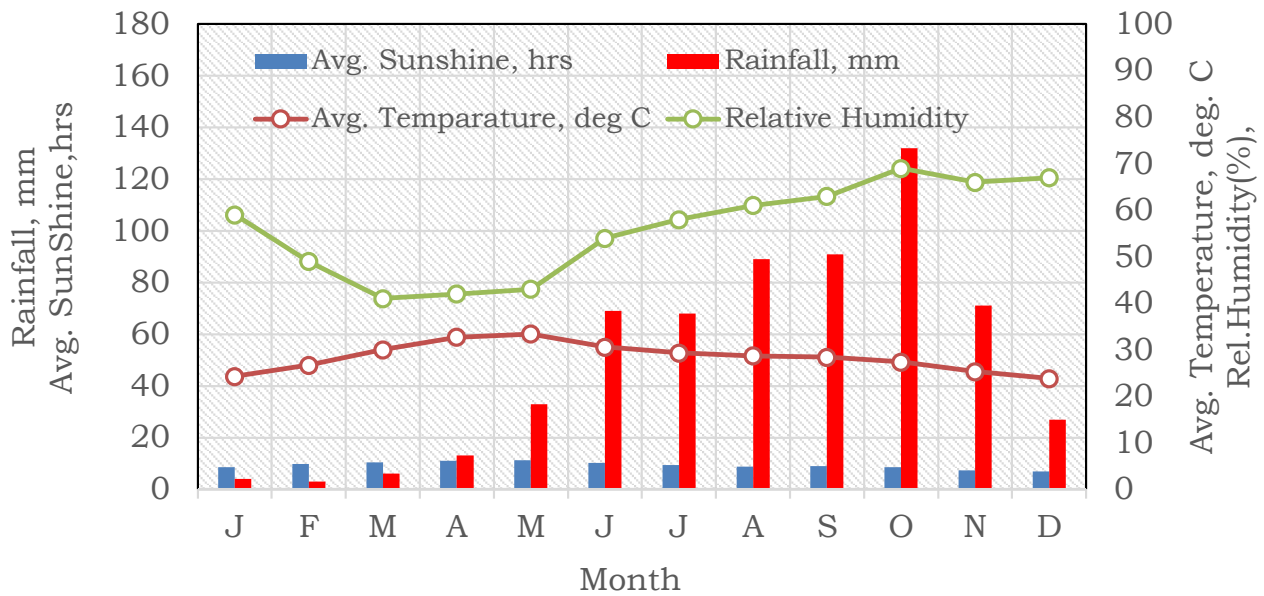


Fig.6: Monthly variation of Rainfall (mm), Average Sunshine (hrs), Average surface Temperature (°C) and Relative Humidity (%).

**3.3 COMPARISON OF MRR AND RADIOSONDE OBSERVATIONS:**

In Fig. 7, monthly average melting layer top height with zero degree isotherm height and monthly variation of temperature (°C) measured from Automatic Weather Station (AWS) observations of 3 (Jan. 2009 to Dec.2011) years is shown.. The height of melting layer varies monthly with a drastic change. The height of melting layer is high in the month of May when compared to the NEM because most of the rain events occurred with lower heights of melting layer. There is presence of melting layer NEM (November, December) because of fog that is predominant in this season. The height of melting layer is directly proportional to the temperatures of the region. Local climate and latitude dependency affect the height of the melting layer. The zero degree isotherm height is found to be well indicated by MRR for both the location. This shows the validity of rain height calculation by MRR. It also indicates the possibility of using MRR effectively for monitoring the zero degree isotherm height in rainy conditions, considering that the Radiosonde launches are not possible in rainy condition.

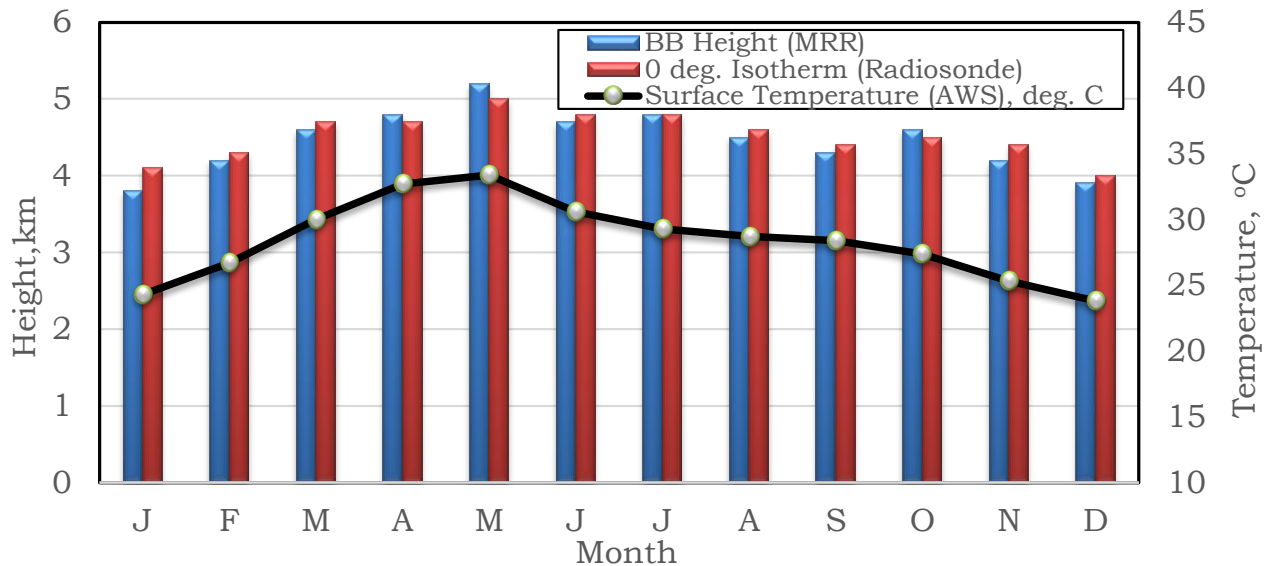


Fig. 7: Monthly mean melting layer top height measured by MRR (2009-2011), radiosonde and monthly mean temperatures at Yogi Vemana University campus, Kadapa.

**3.4. ESTIMATION OF THE RAIN HEIGHT AND IMPLICATION ON ITU-R MODEL**

Rain height which is also known as the freezing height level is the height in which the temperature is at 0°C (the freezing point of water) in a free atmosphere and is often taken to be identical with the ambient 0°C isotherm height (ZDI). It is also the transition height between the lower part of the atmosphere which contains only liquid particles and the upper part containing only freezing particles. Bright-bands which are radar echoes are produced just beneath the 0°C isotherm caused by this melting of ice to water and ice and water has different propagation characteristics. Bright-bands are known to be the thin horizontal layers of enhanced radar reflectivity near the elevation of the melting layer and also a melting layer of ice and snow lying above a Stratiform type of rain which gives an important indication in estimating the height of the Stratiform type of rain and the ZDI (Crane, 1996), (Freeman, 1987). This region in which snow melts into rain often causes a stronger reflectivity than the ice above and rain below (H. E. Green, 2004). Fig. 8 is a typical vertical profile of radar reflectivity showing the position of the bright-band and 0°C isotherm.

The result of the bright-band height based on the measurement from TRMM-PR and MRR is presented in Fig. 9. It could be observed for the two measurements that the bright-band height falls between 4.38km and 4.48 km above mean sea level. It is worth to be stated that even though the measurements are taken using independent equipment, it shows an almost similar pattern of distribution with just about 1.1% differences. Nevertheless, the results reflect the capability of the both instruments with regards to the bright-band height determination prediction in this region.

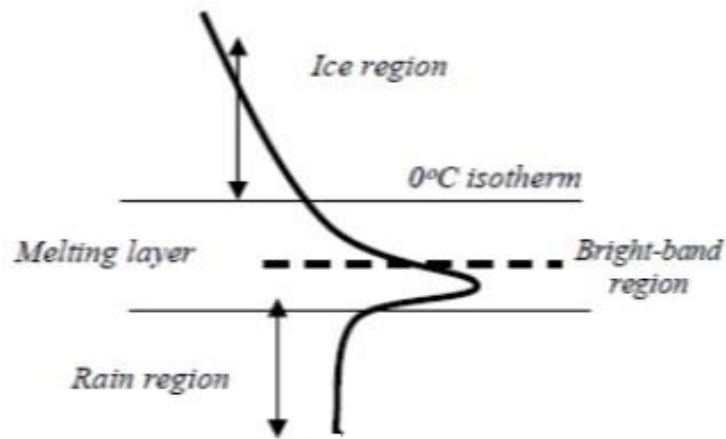


Fig.8: Radar Reflectivity profile displaying the position of melting layer/Bright-band and 0°C isotherm.

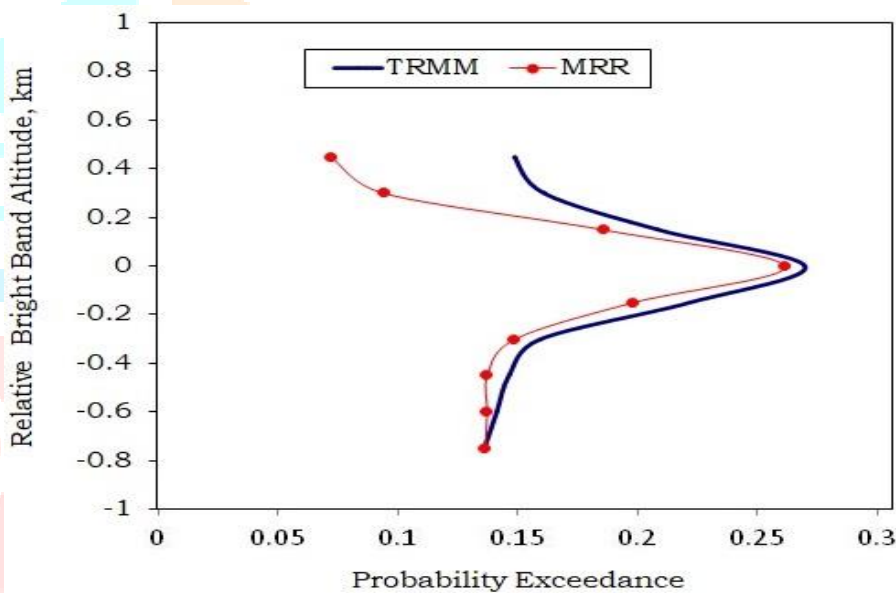


Fig. 9: Comparison of the bright-band height based on the measurement from TRMM-PR and Micro Rain Radar (MRR).

The International Telecommunication Union Radio communication study group -ITU-R. P. 839-3 (Rain height for prediction methods, 2005) gave the rain height to be the height that rain extends during period of precipitation and gave a relation for estimating rain height,  $h_r$ , from the 0°C isotherm as:

$$h_r = h_0 + 0.36 \text{ (km)} \quad \dots (1)$$

where  $h_0$  is the mean 0°C isotherm above the mean sea level.

Figure 10 shows the comparison of rain height from TRMM-PR, the data from MRR observation and ITU-R P.839-3. The rain height by TRMM-PR is computed by assuming that it lies 500 m above the bright-band (J. Awaka et al 2009). It's worth being underlined that an annual mean height of 4.86 km given by the ITU recommendation for this region shows an average percentage difference of about 5% of the measured. This variation is most probably ascribed by the local climatology characteristics in the tropical region which is associated with local convection. In addition, good agreement with each measurements results taken by two independent equipments seems to confirm the reliability of both instruments. As a matter of fact, this result suggests that for proper link design calculation, local values of rain height should be carefully considered.



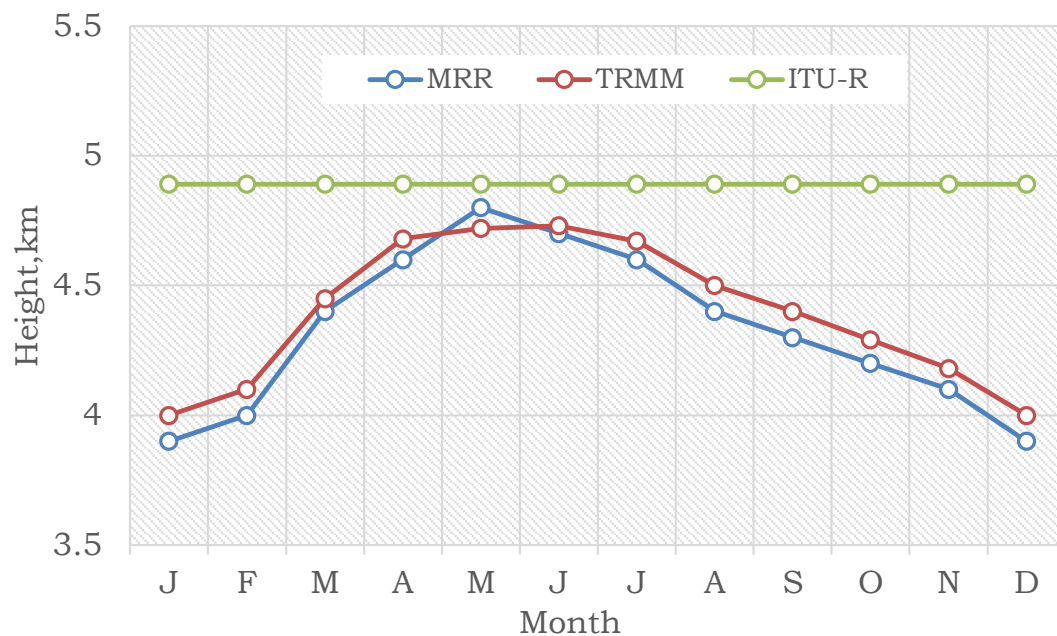


**Fig. 10:** Monthly mean distribution of rain isotherm height obtained from MRR, TRMM-PR and ITU-R P.839-3.

### 3.5 SEASONAL VARIATION OF RAIN HEIGHT WITH RAIN RATE:

To study the variation of melting layer top height with rain rate, the data is categorized in to 0.5 mm/h rain rate bins observed at 200 m height of MRR and averaged over for all 3 years. The variation of top of the melting layer height for SW and NE monsoon has been shown in Fig.11. It shows that the variation in rain height ( $H^0$ ) is quite significant for Stratiform rain during both monsoon regimes. The decreasing pattern of both the curves also implies that it may be a general feature for tropical rains.

The variation is then modeled as linear function of rain rate. The model equations with the coefficient values are given below:

$$H_{SW}^0 = -122.6R + 5121 \quad \text{m.} \quad \dots (2)$$

$$H_{NE}^0 = -222.3R + 5432 \quad \text{m.} \quad \dots (3)$$

The ITU-R model for rain attenuation calculation uses the simple notion of a constant rain height for all rain rate and need to be revised for tropical region. ITU-R P. 618-9 is normally used to calculate the rain attenuation ( $A$ ) from rain rate as follows:

$$A = \gamma L_E \quad \dots (4)$$

Where,  $L_E$  is the path length through rain and  $\gamma$  is the specific rain attenuation. The constant rain height assumption leads to a fixed value of  $L_E$  whereas a rain rate dependent rain height leads to variable path length.

Fig. 12 shows the percentage change in rain attenuation calculation with formal ITU-R model and with the proposed modification for the South-West and North-East monsoon. The percentage change is quite significant with the increase in rain rate, which suggest a possible modification in the ITU-R model.

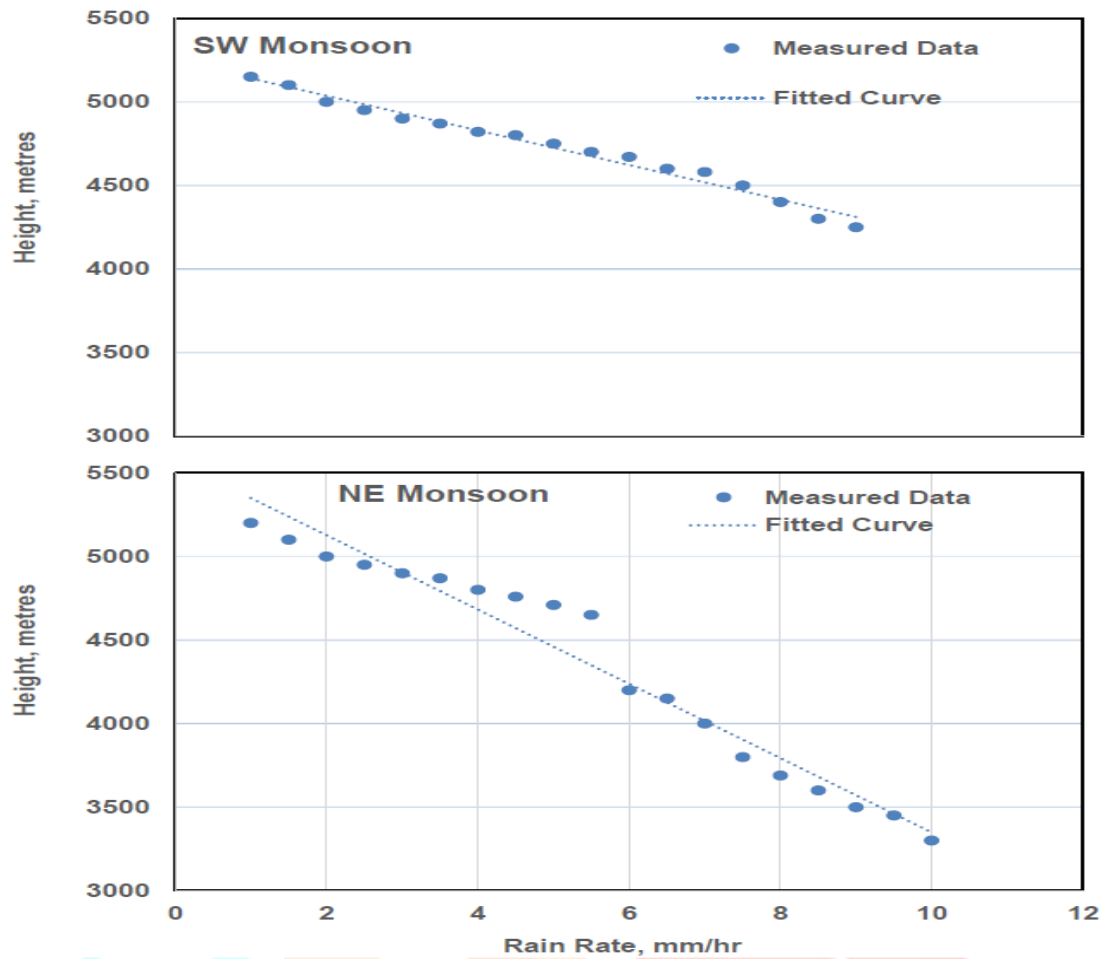


Fig. 11: variation of rain height with rain rate over Kadapa during SW monsoon and NE monsoon

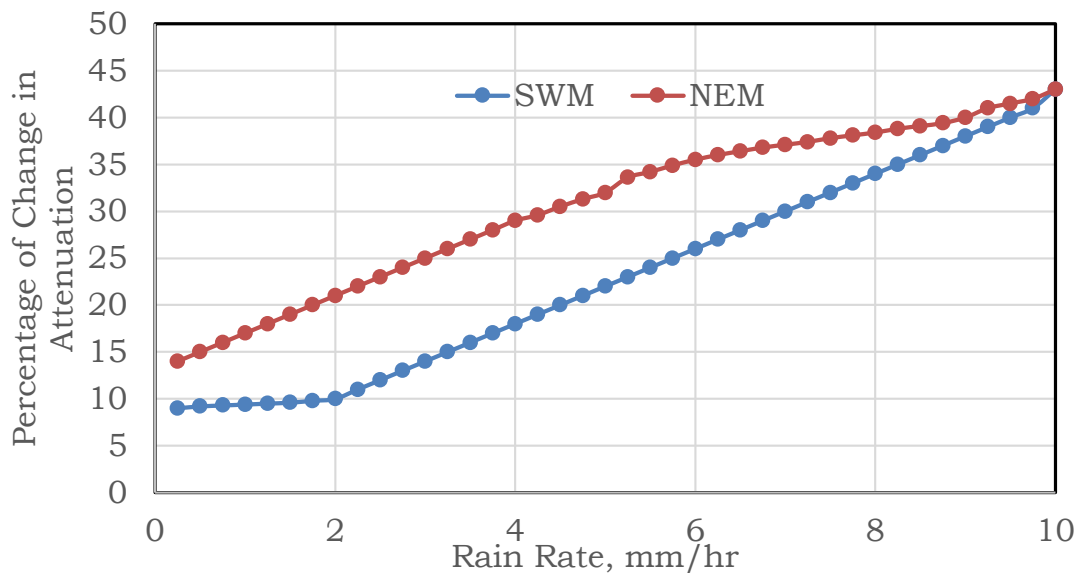


Fig.12: Percentage change in rain attenuation calculated from ITU-R model with fixed rain height and variable rain height during SW and NE Monsoon.

#### IV. CONCLUSION

This paper reports the characteristics of rain height measured by MRR, TRMM-PR and Radiosonde data over Kadapa in tropical semi-arid Indian region. The result shows good agreement between TRMM-PR measurement and ground-based radar observation. It is observed that the melting layer top height measured by MRR is a good indicator of the zero degree isotherm height in rainy condition. The results also highlight the possibility of using MRR for studying the variation of zero degree isotherm in rainy condition when Radiosonde launches are not possible. Rain height for SW monsoon regime shows significant variation than for the NE monsoon regime. However, comparison with the predicted value by the ITU-R shows overestimation of about 5% as compared to the measured value. The study also shows the seasonal dependence effect of the bright-band height in this region. The overall results reveal a careful consideration of local values of rain height for proper link design calculation in order to achieve good quality of services needed by the customers.

## V. ACKNOWLEDGMENTS

Authors are grateful to Indian Space Research Organization (ISRO) for financial support to establish Semi-arid-zonal Atmospheric Research Centre at Yogi Vemana University, Kadapa.

## REFERENCES

- [1] Crane, R. K., Electromagnetic Wave Propagation through Rain, 1st edition, University of Oklahoma, 1996.
- [2] R. L. Freeman, Radio System Design for Telecommunications (1–100 GHz). New York: Wiley, 1987.
- [3] H. E. Green, “Propagation Impairment on Ka-Band SATCOM Links in Tropical and Equatorial Regions”, *IEEE Antennas and Propagation Magazine*, April 2004, Vol. 46, No. 2.
- [4] D.N.Rao, K.Krishna Reddy, K.S.Ravi, S.V.B.Rao, M.J.K.Murthy, H.N.Dutta, S.K.Sarkar, and B.M.Reddy, “A study of Tropospheric Scintillations using Sodar”, *IEE (U.K.) Proceedings Part-H: Microwave Antenna and Propagation*, **138**, 313-318, 1991.
- [5] International Telecommunication Union Recommendation P 618-9: “Propagation data and prediction methods required for design of Earth-space telecommunication systems”, *Propagation in non-ionized media*, 2001, Geneva.
- [6] G. O. Ajayi and F. Barbaliscia, “Prediction of attenuation due to rain: Characteristics of the 0°C Isotherm in temperate and tropical climates”, *Int. J. of Satellite Communications*, 1990, Vol. 8, 187-196.
- [7] D Atlas., R. Srivastava and R Sekhon.: “Doppler radar characteristics of precipitation at vertical incidence”, *Reviews of Geophysics*, February 1973, vol. 11. No. 1, pp 1-35.
- [8] ITU-R P.839-3, “Rain height for prediction methods”, International Telecommunication Union, Geneva Switzerland, 2005.
- [9] U.V.Murali Krishna, K.Krishna Reddy, R.Shirooka, and C.J.Pan, Observational study on Melting layer characteristics over Palau in the Pacific Ocean, *Journal of Atmospheric and Solar-Terrestrial Physics*, **121**, 132--140, 2014, DOI:10.1016/j.jastp.2014.09.015
- [10] G. Peters, B. Fischer and T. Andersson: “Rain observation with a vertically looking Micro Rain Radar (MRR)”, *Boreal environment research*, December 2002, 7, pp 353-362.
- [11] J.Jayalakshmi and K.Krishna Reddy, 2014: Raindrop Size Distributions of South West and North East Monsoon Heavy Precipitations Observed over Kadapa (14° 4' N, 78° 82' E), a Semi-Arid Region of India, *Current Science*, 2014, 107, 1312- 1320
- [12] M. Thurai, E. Deguchi, K. Okamoto and E. Salonen: “Rain Height variability in the tropics”, *IEE Proc.-Microwave, Antennas and Propagation*, 2005, Vol. 152, No. 1.
- [13] J. W. Cha, S.S.Yum, K.H. Chang and S.N. Oh: “Estimation of the melting layer from a Micro Rain Radar (MRR) data at the cloud physics observation system (CPOS) site at Daegwallyeong Weather Station.”, *Journal of the Korean Meteorological Society*, 2007, 43, 1, p77-85.
- [14] W Klaassen., “Radar observations and simulations of the melting layer of precipitation”, *Journal of Atmospheric Science*, 1988, 45, 3741-3753.
- [15] G. Galati, M. Naldi, and M. Ferri, “Reconstruction of the spatial distribution of radar reflectivity of precipitation through linear-inversion techniques” *Radar, Sonar and Navigation*, IEE Proceedings, 143, No. 6, pp. 375- 382, 1996.
- [16] D.N.Rao, K.Krishna Reddy, S.V.B.Rao, K.S.Ravi, and M.J.K.Murthy, Acoustic Sounder Application: Performance of three-line-of-sight microwave links situated over hilly terrains in Southern India, *Int. J. Remote Sensing*, 15, pp.283-292, 1994.
- [17] J.Janapati, B. K. Seela, P.-L. Lin, P.-K. Wang, C.-H. Tseng, K. K. Reddy, H. Hashiguchi, L. Feng, S. K. Das, and C. K. Unnikrishnan, Raindrop size distribution characteristics of Indian and Pacific Ocean tropical cyclones observed at India and Taiwan sites. *J. Meteor. Soc. Japan*, 98, 299–317, doi:10.2151/jmsj.2020-015, 2020.
- [18] S. Das, K. Ashish. and A. Maitra, “Investigation of vertical profile of rain microstructure at Ahmedabad in Indian tropical region”, *Advances in Space Research*, 45, pp. 1235-1243, 2010
- [19] F. Fabry and I. Zawadaki, “Long-term radar observations of melting layer of precipitation and their interpretation” *Journal of Atmos. Sci.* 52, pp. 838-851, 1995.
- [20] K.Krishna Reddy, and T.Kozu, Measurements of raindrop size distribution over Gadanki during south-west and north-east monsoon, *Indian Journal of Radio & Space Physics*, 32, pp. 286-295, 2003
- [21] T.N Rao, D.N Rao, K. Mohan and S. Raghavan, “Classification of tropical precipitation systems and associated Z-R relationships”, *Journal. of Geophys Res*, 106 (D16), pp. 17699-17711, 2001.
- [22] J. Awaka, T. Iguchi, and K. Okamoto, “TRMM PR Standard Algorithm 2A23 and its Performance on Bright Band Detection”, *J. Meteorological Soc. of Japan*. 87A: 31-52. 2009.
- [23] Subrahmanyam, K.V., G. Ramkumar, K.K. Kumar, D. Swain, S.V. SunilKumar, S.S. Das, R.K. Choudhary, K.V.S. Nambodiri, K.N. Uma, S.B. Veena, and A. Babu, 2011: Temperature perturbations in the troposphere–stratosphere over Thumba (8.5°N, 76.9°E) during the solar eclipse 2009/2010, *Ann. Geophys.*, 29, 275–282, [http://dx.doi.org/10.5194/angeo-29-275.\(2011\)](http://dx.doi.org/10.5194/angeo-29-275.(2011)).